REFERENCES

1. Libby P. What have we learned about the biology of atherosclerosis? The role of inflammation. *Am J Cardiol.* 2001;88(7B):3J-6J.
2. Libby P. Inflammation in atherosclerosis. *Nature.* 2002;420(6917):868-874.
3. Zhang Z, Machac J, Helft G, et al. Non-invasive imaging of atherosclerotic plaque macrophage in a rabbit model with F-18 FDG PET: a histopathological correlation. *BMC Nucl Med.* 2006;6:3.
4. Ogawa M, Ishino S, Mukai T, et al. (18)F-FDG accumulation in atherosclerotic plaques: immunohistochemical and PET imaging study. *J Nucl Med.* 2004;45(7):1245-1250.
5. Rudd JH, Warburton EA, Fryer TD, et al. Imaging atherosclerotic plaque inflammation with [18F]-fluorodeoxyglucose positron emission tomography. *Circulation.* 2002;105(23):2708-2711.
6. Fifer KM, Qadir S, Subramanian S, et al. Positron emission tomography measurement of periodontal (18)f-fluorodeoxyglucose uptake is associated with histologically determined carotid plaque inflammation. *J Am Coll Cardiol.* 2011;57(8):971-976.
7. Tawakol A, Migrino RQ, Bashian GG, et al. In vivo 18F-fluorodeoxyglucose positron emission tomography imaging provides a noninvasive measure of carotid plaque inflammation in patients. *J Am Coll Cardiol.* 2006;48(9):1818-1824.
8. Rudd JH, Myers KS, Bansilal S, et al. Atherosclerosis inflammation imaging with 18F-FDG PET: carotid, iliac, and femoral uptake reproducibility, quantification methods, and recommendations. *J Nucl Med.* 2008;49(6):871-878.
9. Rudd JH, Myers KS, Bansilal S, et al. Relationships among regional arterial inflammation, calcification, risk factors, and biomarkers: a prospective fluorodeoxyglucose positron-emission tomography/computed tomography imaging study. *Circ Cardiovasc Imaging.* 2009;2(2):107-115.

10. Chen W, Bural GG, Torigian DA, Rader DJ, Alavi A. Emerging role of FDG-PET/CT in assessing atherosclerosis in large arteries. *Eur J Nucl Med Mol Imaging.* 2009;36(1):144-151.
11. Deichen JT, Prante O, Gack M, Schmiedehausen K, Kuwert T. Uptake of [18F]fluorodeoxyglucose in human monocyte-macrophages in vitro. *Eur J Nucl Med Mol Imaging.* 2003;30(2):267-273.
12. Bucerius J, Mani V, Moncrieff C, et al. Impact of noninsulin-dependent type 2 diabetes on carotid wall 18F-fluorodeoxyglucose positron emission tomography uptake. *J Am Coll Cardiol.* 2012;59(23):2080-2088.
13. Stossel TP. Phagocytosis (first of three parts). *N Engl J Med.* 1974;290(13):717-723.
14. Pratten MK, Lloyd JB. Pinocytosis and phagocytosis: the effect of size of a particulate substrate on its mode of capture by rat peritoneal macrophages cultured in vitro. *Biochim Biophys Acta.* 1986;881(3):307-313.
15. Fadok VA, Voelker DR, Campbell PA, Cohen JJ, Bratton DL, Henson PM. Exposure of phosphatidylserine on the surface of apoptotic lymphocytes triggers specific recognition and removal by macrophages. *J Immunol.* 1992;148(7):2207-2216.
16. Tait JF, Smith C. Phosphatidylserine receptors: role of CD36 in binding of anionic phospholipid vesicles to monocytic cells. *J Biol Chem.* 1999;274(5):3048-3054.
17. Henson PM, Bratton DL, Fadok VA. Apoptotic cell removal. *Curr Biol.* 2001;11(19):R795-805.
18. Oussoren C, Storm G. Liposomes to target the lymphatics by subcutaneous administration. *Adv Drug Deliv Rev.* 2001;50(1-2):143-156.
19. Lindh I, Stawinski J. A general method for the synthesis of glycerophospholipids and their analogs via H-phosphonate intermediates. *J Org Chem.* 1989;54(6):1338-1342.

20. Ogihara-Umeda I, Sasaki T, Kojima S, Nishigori H. Optimal radiolabeled liposomes for tumor imaging. *J Nucl Med.* 1996;37(2):326-332.
21. Mauldin JP, Srinivasan S, Mulya A, et al. Reduction in ABCG1 in Type 2 diabetic mice increases macrophage foam cell formation. *J Biol Chem.* 2006;281(30):21216-21224.
22. Lowry OH, Rosebrough NJ, Farr AL, Randall RJ. Protein measurement with the Folin phenol reagent. *J Biol Chem.* 1951;193(1):265-275.
23. Tsukada T, Rosenfeld M, Ross R, Gown AM. Immunocytochemical analysis of cellular components in atherosclerotic lesions. Use of monoclonal antibodies with the Watanabe and fat-fed rabbit. *Arteriosclerosis.* 1986;6(6):601-613.
24. Ogawa M, Nakamura S, Saito Y, Kosugi M, Magata Y. What can be seen by 18F-FDG PET in atherosclerosis imaging? The effect of foam cell formation on 18F-FDG uptake to macrophages in vitro. *J Nucl Med.* 2012;53(1):55-58.
25. Milla P, Dosio F, Cattel L. PEGylation of proteins and liposomes: a powerful and flexible strategy to improve the drug delivery. *Curr Drug Metab.* 2012;13(1):105-119.
26. Almer G, Wernig K, Saba-Lepek M, et al. Adiponectin-coated nanoparticles for enhanced imaging of atherosclerotic plaques. *Int J Nanomedicine.* 2011;6:1279-1290.
27. Li D, Patel AR, Klibanov AL, et al. Molecular imaging of atherosclerotic plaques targeted to oxidized LDL receptor LOX-1 by SPECT/CT and magnetic resonance. *Circ Cardiovasc Imaging.* 2010;3(4):464-472.
28. Mulder WJ, Douma K, Koning GA, et al. Liposome-enhanced MRI of neointimal lesions in the ApoE-KO mouse. *Magn Reson Med.* 2006;55(5):1170-1174.
29. Torchilin VP. Recent advances with liposomes as pharmaceutical carriers. *Nat Rev Drug Discov.* 2005;4(2):145-160.

Table 1 Biodistribution of [^{111}In]PS100 in normal mice.

Organ	Time after injection (min)					
	1	5	20	60	120	240
Blood	18.4 ± 2.38	1.54 ± 0.31	0.98 ± 0.09	1.01 ± 0.22	0.74 ± 0.15	0.66 ± 0.06
Intestine	0.29 ± 0.06	0.19 ± 0.03	0.23 ± 0.08	0.26 ± 0.05	0.23 ± 0.07	0.42 ± 0.01
Kidney	2.33 ± 0.32	2.84 ± 0.36	3.33 ± 0.49	3.24 ± 0.59	3.49 ± 0.28	4.00 ± 0.29
Liver	34.9 ± 2.60	58.9 ± 6.50	62.6 ± 8.10	62.1 ± 4.16	57.8 ± 8.75	59.3 ± 3.03
Stomach	0.27 ± 0.08	0.53 ± 0.28	0.21 ± 0.06	0.29 ± 0.10	0.31 ± 0.15	0.41 ± 0.17
Spleen	14.3 ± 4.42	42.4 ± 11.4	36.7 ± 7.40	40.9 ± 7.32	42.3 ± 10.9	44.5 ± 4.71
Pancreas	0.50 ± 0.07	0.36 ± 0.01	0.30 ± 0.06	0.48 ± 0.27	0.30 ± 0.06	0.30 ± 0.07
Lung	9.51 ± 3.81	1.49 ± 0.16	0.99 ± 0.10	1.17 ± 0.57	0.72 ± 0.08	0.76 ± 0.12
Heart	2.50 ± 0.64	0.61 ± 0.13	0.46 ± 0.06	0.49 ± 0.09	0.42 ± 0.07	0.44 ± 0.04

*Each value represents mean ± S.D. (%dose/g, n=4 or 5).

Table 2 Biodistribution of [^{111}In]PS200 in normal mice.

Organ	Time after injection (min)					
	1	5	20	60	120	240
Blood	13.1 ± 5.88	3.16 ± 0.55	3.29 ± 0.57	2.92 ± 0.36	2.44 ± 0.50	1.95 ± 0.53
Intestine	0.48 ± 0.12	0.46 ± 0.08	0.44 ± 0.09	0.61 ± 0.16	0.68 ± 0.24	0.86 ± 0.26
Kidney	3.89 ± 1.05	8.98 ± 1.53	9.23 ± 1.96	8.95 ± 1.31	11.0 ± 3.48	12.0 ± 3.07
Liver	22.3 ± 5.96	32.8 ± 5.01	35.2 ± 3.47	36.0 ± 3.30	37.1 ± 6.12	39.1 ± 2.00
Stomach	0.41 ± 0.14	0.38 ± 0.11	0.45 ± 0.06	0.46 ± 0.13	0.39 ± 0.09	0.57 ± 0.22
Spleen	6.05 ± 2.09	20.7 ± 5.73	17.8 ± 5.38	19.0 ± 5.89	21.2 ± 2.96	23.8 ± 5.35
Pancreas	1.05 ± 0.10	0.83 ± 0.14	0.70 ± 0.08	0.83 ± 0.04	0.66 ± 0.11	0.76 ± 0.09
Lung	9.93 ± 2.53	2.59 ± 0.47	2.37 ± 0.35	2.22 ± 0.39	2.14 ± 0.49	1.60 ± 0.36
Heart	2.44± 0.79	1.09 ± 0.17	1.01 ± 0.16	1.11 ± 0.22	0.93 ± 0.15	0.91 ± 0.25

*Each value represents mean ± S.D. (%dose/g, n=4 or 5).

Table 3 Biodistribution of [^{111}In]PC100 in normal mice.

Organ	Time after injection (min)					
	1	5	20	60	120	240
Blood	32.9 ± 4.08	30.1 ± 0.46	17.0 ± 5.99	5.75 ± 4.63	0.52 ± 0.49	1.58 ± 1.96
Intestine	0.40 ± 0.05	0.46 ± 0.06	0.37 ± 0.16	0.28 ± 0.13	0.23 ± 0.10	0.59 ± 0.33
Kidney	3.43 ± 0.50	3.51 ± 0.17	3.02 ± 0.96	2.28 ± 0.99	1.56 ± 0.38	3.39 ± 1.63
Liver	6.34 ± 1.67	12.5 ± 2.66	28.1 ± 6.65	47.2 ± 5.75	53.8 ± 6.85	46.5 ± 13.4
Stomach	0.45 ± 0.14	0.56 ± 0.23	0.43 ± 0.14	0.40 ± 0.16	0.39 ± 0.21	0.44 ± 0.14
Spleen	5.16 ± 2.77	17.9 ± 3.20	101 ± 32.6	171 ± 69.4	174 ± 68.3	193 ± 53.7
Pancreas	0.65 ± 0.14	0.66 ± 0.09	0.54 ± 0.25	0.32 ± 0.21	0.21 ± 0.19	0.84 ± 0.48
Lung	18.9 ± 7.76	11.8 ± 1.51	6.62 ± 1.91	3.48 ± 2.55	0.64 ± 0.50	2.66 ± 2.20
Heart	4.33 ± 0.88	3.31 ± 1.00	2.08 ± 0.76	0.78 ± 0.63	0.19 ± 0.07	0.53 ± 0.54

*Each value represents mean ± S.D. (%dose/g, n=4 or 5).

Table 4 Biodistribution of [^{111}In]PC200 in normal mice.

	Time after injection (min)					
Organ	1	5	20	60	120	240
Blood	33.2 ± 4.03	18.6 ± 5.01	6.83 ± 3.47	2.57 ± 1.33	1.10 ± 0.13	0.65 ± 0.10
Intestine	0.36 ± 0.07	0.31 ± 0.05	0.27 ± 0.03	0.28 ± 0.07	0.32 ± 0.14	0.32 ± 0.09
Kidney	3.35 ± 0.62	3.38 ± 0.51	4.81 ± 1.03	4.38 ± 0.75	4.72 ± 0.67	5.41 ± 1.02
Liver	8.08 ± 2.32	26.7 ± 8.32	38.6 ± 4.17	48.8 ± 3.38	49.4 ± 6.14	46.2 ± 7.84
Stomach	0.54 ± 0.22	0.44 ± 0.16	0.44 ± 0.13	0.40 ± 0.14	0.33 ± 0.20	0.28 ± 0.11
Spleen	10.0 ± 4.24	49.4 ± 12.2	72.2 ± 15.5	112 ± 30.3	142 ± 43.8	173 ± 76.2
Pancreas	0.71 ± 0.27	0.58 ± 0.18	0.44 ± 0.14	0.43 ± 0.10	0.45 ± 0.15	0.38 ± 0.15
Lung	20.8 ± 3.74	9.89 ± 1.79	4.20 ± 1.95	2.00 ± 0.74	1.62 ± 1.02	0.99 ± 0.24
Heart	6.05 ± 2.53	2.95 ± 1.71	1.02 ± 0.39	0.56 ± 0.22	0.49 ± 0.13	0.33 ± 0.07

*Each value represents mean ± S.D. (%dose/g, n=4 or 5).

FIGURE LEGENDS

FIGURE 1.

^{111}In-labeled liposome uptake by cultured macrophages. A significantly higher uptake was observed in PS liposomes compared to PC liposomes of each size (*P<0.05). D isomer of PS liposomes showed lower uptake than L isomers.

Fig. 1

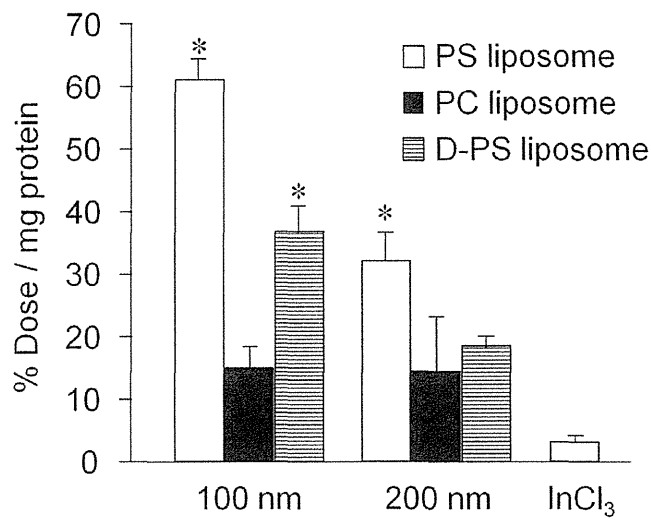

FIGURE 2.

En face autoradiography of ApoE -/- mice aorta. Photographic images of unstained aorta (A), images after Oil Red O staining (B), autoradiograms (C), and target-to-nontarget ratio (TNR) (D). The autoradiograms were well matched with Oil Red O staining. TNR was significantly higher in PS liposomes than PC liposomes in each size (*P<0.05). PS200 showed higher TNR than PS100 (†P<0.05).

Fig. 2

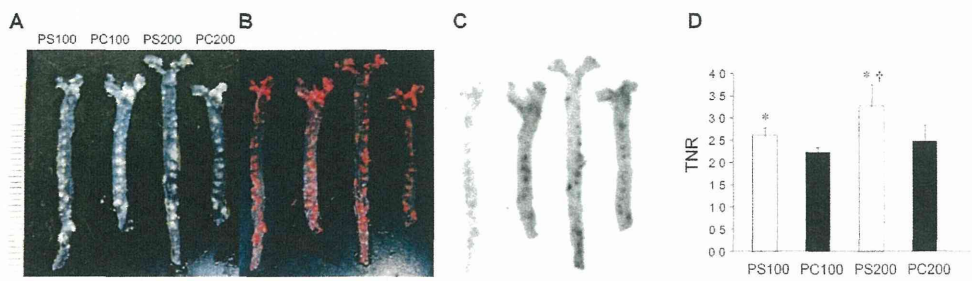

FIGURE 3.

SPECT and CT images, *ex vivo* ARG, and histological images of [^{111}In]PS100 (A) and [^{111}In]PS200 (B) in WHHL rabbits, and [^{111}In]PS200 in a normal rabbit (C). The white arrows indicate the position of the aorta. "L" represents the liver. Magnified images of Azan-Mallory staining show a macrophage foam cell-rich region with less smooth muscle cells (dashed red circle), and a more fibrotic region with dead macrophages (dashed yellow circle). The atherosclerotic regions were successfully visualized with [^{111}In]PS200 and [^{111}In]PS100 in WHHL rabbits. The radioactivity was accumulated in macrophage foam cell area, and was low in the fibrotic area. No aortic accumulation was seen in a normal rabbit.

Fig. 3